AMERICAN SOCIETY FOR MICROBIOLOGY | Journal of Bacteriology®

RESEARCH ARTICLE

Redirection of Metabolism in Response to Fatty Acid Kinase in *Staphylococcus aureus*

Zachary DeMars,[a] Jeffrey L. Bose[a]

[a]Department of Microbiology, Molecular Genetics and Immunology, University of Kansas Medical Center, Kansas City, Kansas, USA

ABSTRACT *Staphylococcus aureus* is capable of phosphorylating exogenous fatty acids for incorporation into the bacterium's membrane via the fatty acid kinase, FakA. Additionally, FakA plays a significant role in virulence factor regulation and skin infections. We previously showed that a *fakA* mutant displays altered growth kinetics *in vitro*, observed during the late-exponential phase of growth. Here, we demonstrate that the absence of FakA leads to key metabolic changes. First, the *fakA* mutant has an altered acetate metabolism, with acetate being consumed at an increased rate than in the wild-type strain. Moreover, the growth benefit was diminished with inactivation of the acetate-generating enzyme AckA. Using a mass spectrometry-based approach, we identified altered concentrations of tricarboxylic acid (TCA) cycle intermediates and both intracellular and extracellular amino acids. Together, these data demonstrate a change in carbohydrate carbon utilization and altered amino acid metabolism in the *fakA* mutant. Energy status analysis revealed the mutant had a similar ADP/ATP ratio to that of the wild type, but a reduced adenylate energy charge. The inactivation of *fakA* changed the NAD^+/NADH and $NADP^+$/NADPH ratios, indicating a more oxidized cellular environment. Evidence points to the global metabolic regulatory proteins CcpA and CodY being important contributors to the altered growth in a *fakA* mutant. Indeed, it was found that directing amino acids from the urea cycle into the TCA cycle via glutamate dehydrogenase was an essential component of *S. aureus* growth after glucose depletion. Together, these data identify a previously unidentified role of FakA in the global physiology of *S. aureus*, linking external fatty acid utilization and central metabolism.

IMPORTANCE The fatty acid kinase, FakA, of *Staphylococcus aureus* plays several important roles in the cell. FakA is important for the activation of the SaeRS two-component system and secreted virulence factors like α-hemolysin. However, the contribution of FakA to cellular metabolism has not been explored. Here, we highlight the metabolic consequence of removal of FakA from the cell. The absence of FakA leads to altered acetate metabolism and altered redox balance, as well as a change in intracellular amino acids. Additionally, the use of environmental amino acid sources is affected by FakA. Together, these results demonstrate for the first time that FakA provides a link between the pathways for exogenous fatty acid use, virulence factor regulation, and other metabolic processes.

KEYWORDS FakA, metabolism, acetate metabolism, metabolomics, *Staphylococcus*

The facultatively anaerobic Gram-positive bacterium *Staphylococcus aureus* is a common colonizer of the human nares but is also a potent human pathogen. While primarily causing skin infections, *S. aureus* is capable of establishing infection in a multitude of anatomical sites in the human body, leading to life-threatening diseases (1). These different niches have a wide variety of nutrients, necessitating *S. aureus* to

Received 7 June 2018 **Accepted** 6 July 2018

Accepted manuscript posted online 16 July 2018

Citation Demars Z, Bose JL. 2018. Redirection of metabolism in response to fatty acid kinase in *Staphylococcus aureus*. J Bacteriol 200:e00345-18. https://doi.org/10.1128/JB.00345-18.

Editor Ann M. Stock, Rutgers University-Robert Wood Johnson Medical School

Address correspondence to Jeffrey L. Bose, jbose@kumc.edu.

have an adaptable metabolism. Perhaps, not surprisingly, virulence factor production and metabolism are linked as *S. aureus* adapts to its environment (2, 3).

S. aureus possesses complete central metabolic pathways, including glycolysis, the pentose phosphate pathway, and the tricarboxylic acid (TCA) cycle. These metabolic pathways, as well as virulence factor production, are under the control of global regulators (3–6). Carbon catabolite protein A, or CcpA, is a DNA-binding protein and has been shown to regulate multiple branches of metabolism. Importantly, CcpA represses the TCA cycle in the presence of glucose or other glycolytic carbohydrates that generate fructose-1,6-bisphosphate (7–11). In addition, CcpA controls the expression of genes encoding key enzymes in amino acid metabolism (5, 12, 13). CodY is a global transcriptional regulator that directly monitors the intracellular concentrations of branch-chained amino acids (BCAAs), as well as levels of cellular GTP (14, 15). Accordingly, CodY has been shown to regulate BCAA biosynthesis pathways and control a multitude of virulence factors, from repressing toxins to activating microbial surface components recognizing adhesive matrix molecules (MSCRAMMs) (4, 16–18). Deletion of *ccpA* from *Staphylococcus aureus* impacts the transcription of virulence factors, such as the downregulation of the global effector molecule of the Agr system, RNAIII (19). CodY has also been shown to alter transcription of the *agr* locus and thus expression of virulence factors such as α-hemolysin (4, 20, 21). More recently, CodY binding motifs were identified upstream of the P1 promoter of the *saePQRS* operon (22), suggesting a direct role for CodY regulating secreted virulence factors. As a consequence of these two key regulatory proteins, both the availability of carbohydrates and amino acids can induce metabolic changes as well as altering virulence factor production.

The details of carbon flow, particularly from glucose, through central metabolism have been a topic of significant study. In the presence of a preferred carbohydrate, such as glucose, *S. aureus* uses glycolysis to produce pyruvate, which can be converted into multiple metabolites depending on the environment. Under aerobic conditions and in the presence of glucose, the TCA cycle is repressed by CcpA (11), and much of the pyruvate is converted to acetyl coenzyme A (acetyl-CoA) and then acetate, with ATP created by substrate-level phosphorylation by the phosphotransacetylase-acetate kinase (Pta-AckA) pathway (23, 24). Once glucose and glycolytic intermediates (fructose-1,6-bisphosphate) are depleted from the environment, CcpA repression of the TCA cycle is relieved and acetate is reassimilated to acetyl-CoA (25) and subsequently processed through the TCA cycle. This switch from acetate production to acetate consumption is known as the "acetate switch" (26), the timing of which is presumably controlled by CcpA both directly and indirectly.

Recently, *fakA* (originally named *vfrB*) was characterized in *Staphylococcus aureus* (27). This gene encodes a fatty acid kinase, which is responsible for phosphorylating exogenous fatty acids and incorporating them into the *S. aureus* phospholipid bilayer (28). FakA has been shown to regulate virulence factor production, such as that of α-hemolysin and several proteases (27), as well as impacting the type VII secretion system (29). We have shown that FakA mediates at least some of these effects through the activation of the SaeRS two-component system (30). In addition, FakA influences biofilm formation (31) by an unknown mechanism. Previously, we showed that deletion of the *fakA* gene led to altered growth kinetics (27). Here, we demonstrate that a *fakA* mutant displays an altered acetate switch as well as an apparent altered amino acid metabolism.

RESULTS

A *fakA* mutant displays altered growth and acetate kinetics. Previously, we showed that a *fakA* mutant has an extended exponential phase of growth, resulting in higher growth yield (27) and suggesting an altered metabolism in the *fakA* mutant. For a summary of metabolic pathways and changes observed in the *fakA* mutant, see Fig. 10. To determine the effect that FakA has on the growth of *S. aureus*, the wild type, the *fakA* mutant, and the *fakA* complemented strain were grown in tryptic soy broth (TSB) supplemented with 14 mM glucose. In agreement with our previous results, we

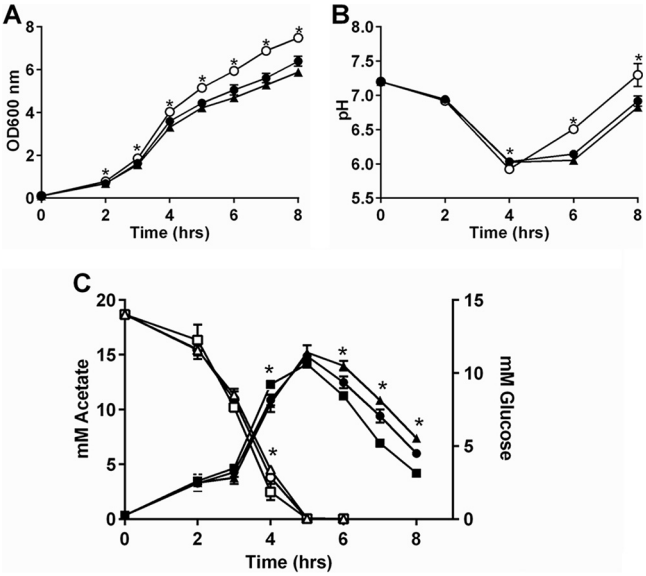

FIG 1 (A) Growth of wild-type (closed circle), *fakA* mutant (open circle), and *fakA* complement (triangle) strains in TSB plus 14 mM glucose at a 1:10 medium-to-flask ratio. (B) pH of culture from panel A. Data are the averages ($n = 3$) with standard deviations from representative experiments. All points have error bars, which may be smaller than symbols. (C) Extracellular acetate (closed symbols) and glucose (open symbols) were determined for wild-type (circles), *fakA* mutant (squares), and complement strains (triangles). Data are averages ($n = 6$) with standard deviations. An asterisk denotes significance (*t* test, $P < 0.05$) compared to the wild type.

observed enhanced late-exponential-phase growth in the *fakA* mutant, which could be restored to wild-type levels when *fakA* was provided on a plasmid (Fig. 1A). Under aerobic growth in the presence of glucose, *S. aureus* produces acetate as a by-product, which leads to decreased medium pH, followed by consumption of acetate and a rise in pH (24, 32, 33). Interestingly, altered growth kinetics of the *fakA* mutant correlated with an increased culture pH (Fig. 1B), consistent with decreased production or enhanced utilization of acetate in the *fakA* mutant. Growing the *fakA* mutant under decreased flask-to-medium ratios resulted in no significant growth advantage compared to the wild-type strain (see Fig. S1A in the supplemental material). Furthermore, the growth advantage observed in the *fakA* mutant was diminished during the exponential phase of growth when grown in TSB lacking glucose, with growth returning to wild-type levels (Fig. S1B). To determine if the growth advantage was due to altered acidification of the medium, the wild type, the *fakA* mutant, and the complemented strain were grown in TSB buffered to a pH of 7.2 with 50 mM morpholinepropanesulfonic acid (MOPS) (Fig. S1C). All strains grew similarly to those grown in unbuffered media, indicating that this growth phenotype is not the result of medium pH changes. Taken together, these data suggest that FakA alters bacterial growth at the exponential phase of growth in a glucose- and oxygen-dependent manner indicative of changes in the acetate switch.

Altered acetate production and the timing of the growth divergence between the wild-type and *fakA* mutant strains correlates with previous studies showing the switch from glucose to acetate utilization in *S. aureus* (32, 33). To directly examine whether glucose to acetate conversion and subsequent acetate consumption are altered in the *fakA* mutant, both acetate and glucose concentrations were determined (Fig. 1C). In agreement with previous work (33), glucose was consumed in the early exponential phase, with a corresponding increase in acetate levels until glucose was depleted. The *fakA* mutant consumed more glucose by hour 4, which corresponded with a slight increase in acetate production and to the start of the growth divergence. During the course of enhanced growth of the *fakA* mutant, decreased levels of acetate were present in the medium, correlating to the observations of increased pH shown in

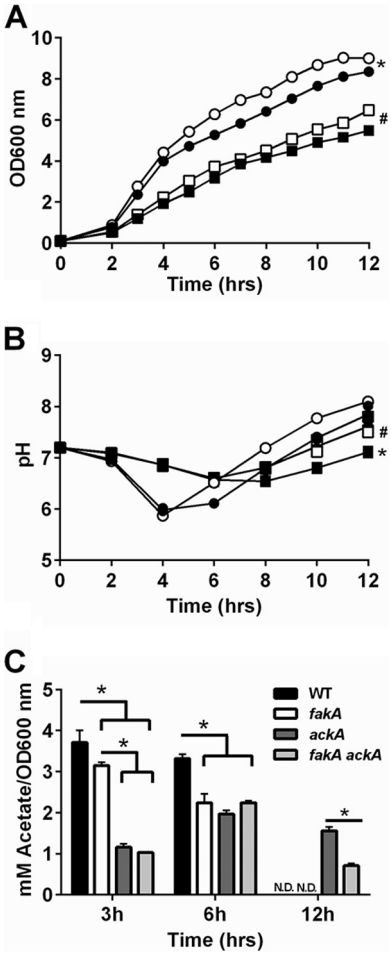

FIG 2 (A) Growth of wild-type (closed circle), *fakA* mutant (open circles), *ackA* mutant (closed square), and *fakA ackA* mutant (open square) strains. An asterisk denotes a significant difference ($P < 0.05$) for all points after 2 h for wild type (WT) versus the *fakA* mutant, while # indicates significance for hours 4, 5, and 9 to 12 for the *ackA* mutant versus the *fakA ackA* mutant. (B) pH of culture media from panel A. An asterisk denotes a significant difference ($P < 0.05$) for all points after 2 h for WT versus the *ackA* mutant, while # identifies differences ($P < 0.05$) for all points after 2 h, except for the *ackA* mutant versus the *fakA ackA* mutant (6 h). (C) Quantification of acetate in the culture media at indicated time points. An asterisk denotes a significant difference ($P < 0.05$). N.D., none detected. For all panels, data are the averages ($n = 3$) with standard deviations from representative experiments. All points have error bars, which may be smaller than symbols.

Fig. 1B. The changes in glucose and acetate utilization were both restored when *fakA* was provided on a plasmid. Together, these results demonstrate that glucose and acetate metabolism is different in the *fakA* mutant, and their timing suggests an altered acetate switch.

Altered growth of the *fakA* mutant is dependent on AckA. Along with the observation of altered acetate levels in the *fakA* mutant compared to those in the wild type, we predicted that the altered growth of a *fakA* mutant would involve the Pta-AckA and AcsA pathways, which are the primary mechanism to produce (33) and consume (25) acetate, respectively. Not surprisingly, the *ackA* and *fakA ackA* mutant strains grew poorly compared to both the wild type and the *fakA* mutant (Fig. 2A). This agrees with previous studies that highlighted the importance of the production of energy from the Pta-AckA pathway in *S. aureus* (13, 32, 34). However, the growth (Fig. 2A) was similar in the *fakA ackA* mutant compared to that of the *ackA* mutant, indicating that the enhanced growth of the *fakA* mutant during the exponential phase of growth is reliant on AckA. The *fakA ackA* mutant did have modest increased growth compared to the *ackA* mutant at several time points. First, a slightly enhanced growth

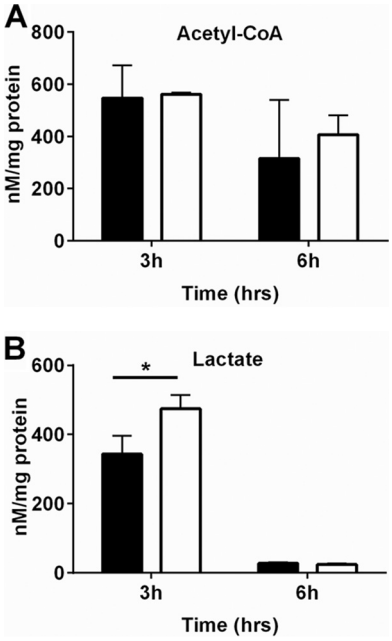

FIG 3 Quantification of intracellular levels of acetyl-CoA (A) and lactate (B) after 3 and 6 h of growth for wild-type (black bars) and *fakA* mutant (white bars) strains. Data are averages ($n = 4$) with standard deviations and are normalized to protein concentration. An asterisk denotes a significant difference (*t* test, $P < 0.05$) compared to the wild type.

was observed at 4 and 5 h of growth, similar to that seen with the *fakA* mutant compared to the wild type in the absence of glucose (Fig. S1B), as well as at the latest time points examined. As seen in a previous report (33), the *ackA* mutants did produce some acetate (Fig. 2C). There was no difference in acetate between the *ackA* and *fakA ackA* mutant at either 3 or 6 h of growth, although the *fakA ackA* mutant consumed more acetate by 12 h. This could be responsible for the increased growth observed in the *fakA ackA* mutant compared to that in the *ackA* mutant (Fig. 2). Current models suggest AcsA as the means to assimilate acetate for redirection into the TCA cycle (24, 25), although experimental confirmation is lacking. Surprisingly, *acsA* and *fakA acsA* mutants resembled the wild type and the *fakA* mutant, respectively, during most of growth (see Fig. S2 in the supplemental material). AcsA had a modest effect in both strains after 8 h, well past the point of glucose exhaustion from the media. Interestingly, the *acsA* mutant depleted approximately 75% of produced acetate (Fig. S2; compare *ascA* at 3 and 12 h). Much like the parent strains, the *fakA acsA* mutant had less acetate in the medium compared to the *acsA* mutant. These data demonstrate a role for acetate produced via AckA in the enhanced growth of the *fakA* mutant, but, in contrast to most models, the majority of acetate is being depleted via another mechanism rather than by the AcsA pathway.

The *fakA* mutant has altered central metabolites, while maintaining acetyl-CoA levels. Alterations in carbon flow through acetate metabolism would likely change additional metabolic processes. To assess other metabolic changes in the *fakA* mutant, we used liquid chromatography-tandem mass spectrometry (LC-MS/MS) to quantify key metabolic intermediates at 3 or 6 h of growth. Pyruvate levels were below the limit of detection (~1 nM mg^{-1} protein) for both the wild-type and *fakA* mutant strains at either time point (data not shown). Acetyl-CoA was readily detected, and there was no significant difference between the strains (Fig. 3A), demonstrating that despite differences in growth kinetics and altered acetate metabolism, acetyl-CoA levels are maintained. Since acetate levels, but not those of acetyl-CoA, were altered in the *fakA* mutant, we suspected that carbon was being shuttled to alternative metabolites. We found that the *fakA* mutant had a 38.3% increase in intracellular lactate compared to

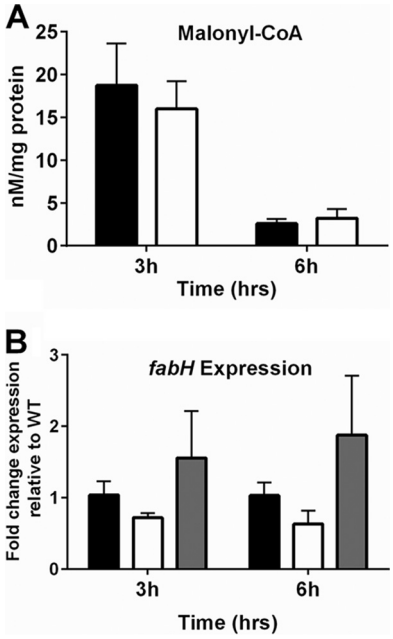

FIG 4 (A) Quantification of intracellular levels of malonyl-CoA after 3 and 6 h of growth for wild-type (black bars) and *fakA* mutant (white bars) strains. Data are averages ($n = 4$) with standard deviations and are normalized to protein concentration. *, $P < 0.05$. (B) *fabH* transcript levels at 3 and 6 h of growth in wild-type (black bars), *fakA* mutant (white bars), and *fakA* complement (gray bars) strains. Data are average ($n = 3$) fold changes relative to wild-type, with standard errors of the mean.

that in the wild type at 3 h of growth but showed no difference at 6 h (Fig. 3B). Although not statistically significant, we also identified increased lactate in the supernatants of the *fakA* mutant compared to those of the wild-type strain (see Table S1 in the supplemental material). However, lactate production was not a major contributing factor to growth, as the growth and pH of *ldh1*, *fakA ldh1*, *ldh2*, and *fakA ldh2* mutants showed no significant differences (see Fig. S3 in the supplemental material). In addition, mutation of *alsS*, which produces acetoin from pyruvate, did not alter growth of the wild type or the *fakA* mutant (Fig. S3).

Since FakA is necessary for exogenous fatty acid use, we tested whether the endogenous fatty acid synthesis system was altered. This is also one direction in which acetyl-CoA is diverted. We found no difference in levels of malonyl-CoA, the intermediate that feeds into fatty acid biosynthesis, between the wild-type and *fakA* mutant strains (Fig. 4A). We also determined the transcription levels for *fabH*, which encodes a key enzyme in fatty acid synthesis (35, 36). In agreement with unaltered malonyl-CoA, *fabH* expression was not significantly changed in the absence of *fakA* (Fig. 4B), indicating that the absence of *fakA* does not affect the endogenous fatty acid synthesis pathway.

One major fate for acetyl-CoA is the TCA cycle. Indeed, when glucose from the environment is exhausted, acetate is converted to acetyl-CoA for use in the TCA cycle. Therefore, we examined the concentrations of several key TCA cycle intermediates. Succinate, fumarate, and malate levels were not significantly different between the wild type and the *fakA* mutant after 3 or 6 h of growth (Table S1). Compared to the wild type, the *fakA* mutant had decreased intracellular citrate and α-ketoglutarate early in growth, but significantly increased levels during the enhanced growth (6 hours). For the full list of quantified organic acids, see Table S1.

The *fakA* mutant has a modified redox state. During growth utilizing glucose, wild-type cells make most of their ATP through substrate phosphorylation via acetate production. Following glucose exhaustion, generation of ATP then shifts to the TCA cycle and electron transport chain. Given that acetyl-CoA levels were unaltered in the

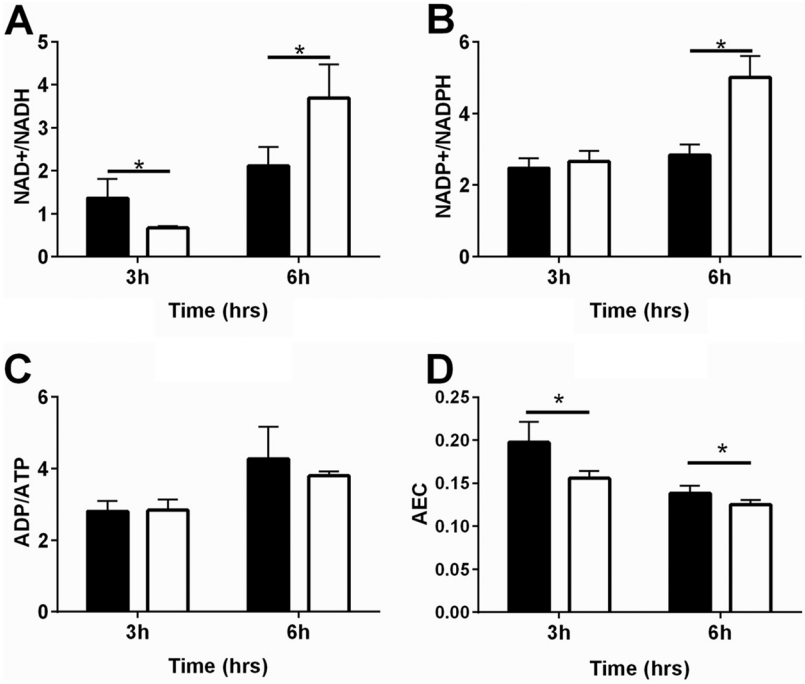

FIG 5 Cellular ratios of NAD^+/NADH (A), $NADP^+$/NADPH (B), and ADP/ATP (C) and adenylate energy charge (AEC) (D) determined by LC-MS/MS after 3 and 6 h of growth for wild-type (black bars) and *fakA* mutant (white bars) strains. Data are the average ratios ($n = 4$) with standard deviations after normalization to protein concentration. An asterisk denotes a significant difference (on *t* test, $P < 0.05$) compared to the wild type.

fakA mutant compared to those of the wild type, we examined the redox and energy state of the cells using LC-MS/MS. After 3 h of growth, the *fakA* mutant displayed a significant decrease in the NAD^+/NADH ratio compared to that of the wild type (Fig. 5A), which transitioned to a significantly increased ratio during enhanced growth (6 h) (Fig. 5A). While no difference was observed for $NADP^+$/NADPH at 3 h of growth, at 6 h, this ratio was increased in the *fakA* mutant compared to that in the wild type (Fig. 5B), and this is attributed to increased $NADP^+$ at this time. Interestingly, at 6 h of growth, the *fakA* mutant had increased levels of both ADP and ATP (see Table S2 in the supplemental material), yet the ADP/ATP ratio was similar to that of the parent strain (Fig. 5C). Additionally, AMP levels were significantly increased in the *fakA* mutant (Table S2). We also used the ATP, ADP, and AMP results to calculate the adenylate energy charge (AEC), as described by Atkinson et al. (37). Using this analysis, the *fakA* mutant was found to have a decreased AEC at both time points examined (Fig. 5D). Together, these data indicate that during enhanced growth, the *fakA* mutant has a more oxidized cellular environment than that of the wild-type strain and has an overall moderately decreased cellular energy status. For the full list of quantified nucleotides, see Table S2.

FakA modulates amino acid metabolism. Recently, Halsey et al. (13) reported that different amino acids play unique roles for bacterial growth in the absence of glucose. For example, the amino acids glutamate, glutamine, proline, arginine, asparagine, and aspartate were shown to provide the organism with TCA cycle intermediates like α-ketoglutarate and oxaloacetate. The amino acids alanine, glycine, and threonine are converted to pyruvate and acetate via the Pta-AckA pathway (13). We sought to determine the amino acid profiles of both wild-type and the *fakA* mutant strains, as they may reflect the altered metabolism observed in the mutant strain. When analyzing cellular amino acids at either 3 or 6 h of growth, we identified significant changes in 15 out of 22 amino acids tested at one or both time points, demonstrating significant changes to amino acid metabolism in the *fakA* mutant (Fig. 6).

Amino acids that can be converted to pyruvate were less abundant in *fakA* mutant cells. Specifically, threonine, glycine, and alanine were all at reduced levels at 6 h in the

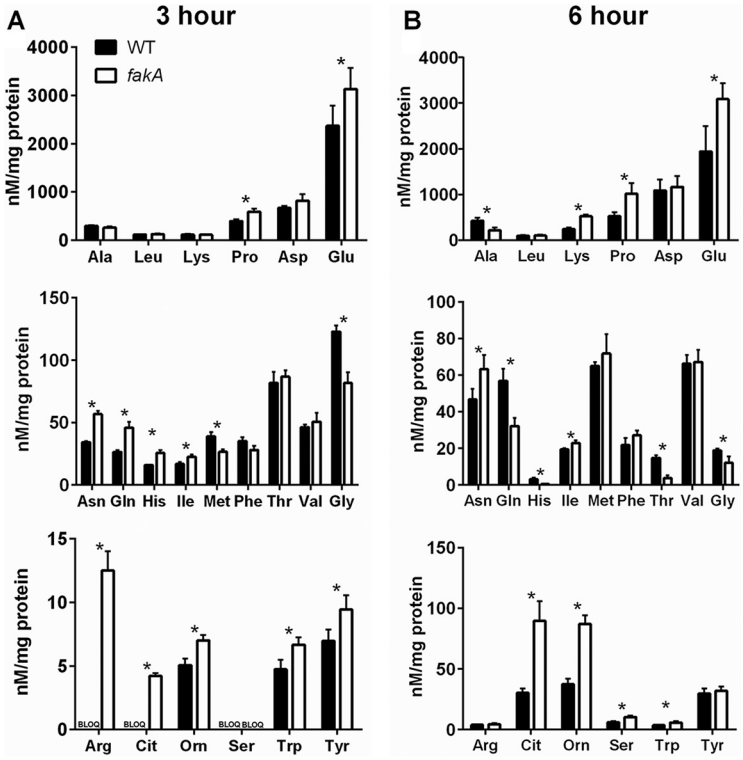

FIG 6 Quantification of intracellular amino acids from wild-type (WT) and *fakA* mutant strains grown for 3 (A) or 6 h (B). Concentrations were normalized to protein concentration. Data are averages ($n = 4$) with standard deviations from representative experiments. An asterisk denotes a significant difference (*t* test, $P < 0.05$) compared to the wild type. BLOQ, concentration below the limit of quantification.

fakA mutant (Fig. 6). These same amino acids were consumed from the media at a greater rate when the starting levels in the media were compared to those of the supernatants. We also observed significant changes in amino acids that are involved in the urea cycle. Intracellular arginine, histidine, proline, and glutamate levels (Fig. 6) were all increased in the *fakA* mutant after 3 h of growth compared to those in the wild type. At 6 h, arginine levels were similar in the wild type and the *fakA* mutant, while histidine levels were lower. At this same time, proline and glutamate levels were increased in the mutant.

Two nonproteinogenic amino acids were also examined. Citrulline and ornithine are amino acids involved in the urea cycle, which is a key pathway in amino acid catabolism and allows available carbon to enter the TCA cycle via α-ketoglutarate. After three and 6 h of growth, citrulline and ornithine levels were significantly increased in the *fakA* mutant compared to those in the wild type (Fig. 6), suggesting altered urea cycle activity. Therefore, we hypothesized that urease activity would be impacted. The urea cycle connects glutamate and amino acids producing glutamate to the TCA cycle and is subjected to carbon catabolite regulation independently of the presence of glucose (11, 12). Urease activity was determined after 3 and 6 h of growth. The activity of urease was increased in the *fakA* mutant compared to that in the wild type at both time points (Fig. 7A). This is likely due to increased urease levels, since in the *fakA* mutant we observed increased expression of a β-galactosidase-based reporter of the urease promoter (Fig. 7B). Despite this increase in urease activity, inactivation of urease in both wild-type and *fakA* mutant strains did not alter growth under our conditions (data not shown).

Global regulators CcpA and CodY alter growth of the *fakA* mutant. The altered growth of the *fakA* mutant is observed as glucose is depleted from the medium. Since CcpA carries out its regulation in a glucose-dependent manner, we reasoned that CcpA

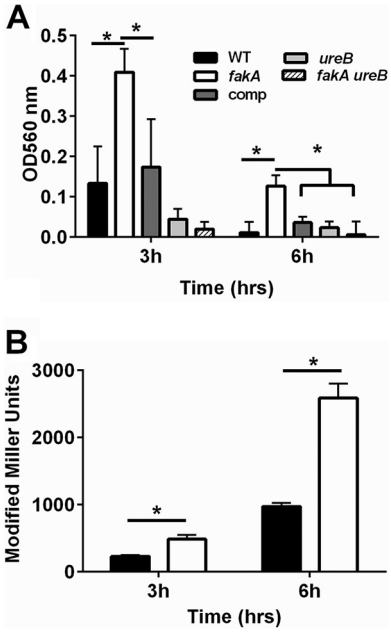

FIG 7 (A) Urease activity was determined via absorbance at 560 nm for indicated strains grown for 3 or 6 h. (B) β-Galactosidase activity from a P_{ure}-*lacZ* reporter measured in wild-type (black bars) and *fakA* mutant (white bars) strains grown for 3 or 6 h. All data are the averages ($n = 3$) with standard deviations from representative experiments. An asterisk denotes a significant difference (*t* test, $P < 0.05$).

may have a role in the *fakA* mutant's altered growth. Therefore, growth was monitored in the absence of *ccpA*. After glucose depletion from the media, the *ccpA* and *fakA ccpA* mutants grew similarly to the *fakA* mutant and better than the wild-type strain (Fig. 8A). One indicator of CcpA activity is expression of *gltA*, which is repressed by CcpA (11). To assess potential alterations in CcpA activity, *gltA* mRNA levels were assessed after 3 and 6 h of growth. Interestingly, while glucose was present, transcription of *gltA* was increased 2-fold in the *fakA* mutant compared to that in the wild type, but it decreased upon glucose exhaustion (6 h), similarly to that in a *ccpA* mutant (Fig. 8B). This result indicates that CcpA activity may be altered in the *fakA* mutant.

We observed differences in amino acid metabolism (see Table S3 in the supplemental material) and guanine-based nucleotides (Table S2), both of which alter CodY activity. In addition, amino acids are abundant in TSB, and it was possible that enhanced growth was due in part to amino acid utilization. Due to the role of CodY in regulating amino acid metabolism, we hypothesized that it may affect growth of the *fakA* mutant. Indeed, inactivation of *codY* in the *fakA* mutant diminished the growth of the *fakA* mutant to near wild-type levels, whereas the single *codY* mutant displayed no altered growth (Fig. 8C). CodY is known to repress expression of *ilvD* (38); we therefore used this transcript as an indicator of CodY activity. After 3 h, *ilvD* expression was not significantly altered in the *fakA* mutant compared to that in the wild type (Fig. 8D). Surprisingly, *ilvD* expression was reduced in the absence of *codY* and *fakA* together compared to that in the *codY* mutant alone.

GudB is necessary for growth post-glucose consumption. Glutamate dehydrogenase, encoded by *gudB*, produces α-ketoglutarate from glutamate, linking the urea cycle amino acids to central metabolism (13). Since we observed altered urease activity and amino acids levels associated with the urea cycle in the *fakA* mutant, we hypothesized that directing carbon from these pathways into central metabolism would be important for the growth of the *fakA* mutant. This is also suggested by the increased α-ketoglutarate levels observed in the *fakA* mutant (Table S1). Indeed, mutation of *gudB* hindered growth of both the wild-type and *fakA* mutant strains (Fig. 9A). Likewise, the pH of the media was not different between the *gudB* and *fakA gudB* mutants (Fig. 9B).

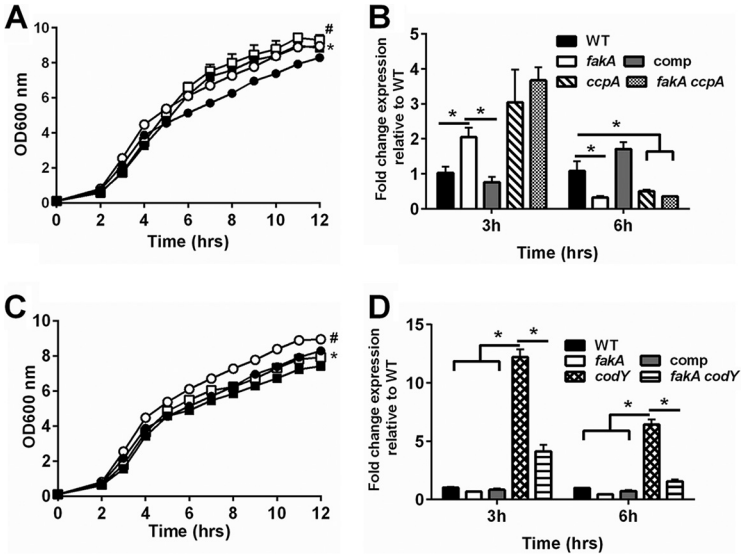

FIG 8 (A) Growth of wild-type (closed circle), *fakA* mutant (open circle), *ccpA* mutant (closed square), and *fakA ccpA* mutant (open square) strains. All data points are the averages ($n = 3$) with standard deviations from representative experiments. An asterisk indicates a significant difference ($P < 0.05$) between the WT and *ccpA* mutant for all time points except 5 h, and # indicates significant difference between the *fakA* and *fakA ccpA* mutants at hours 2 to 4 and 11 only. (B) Transcript levels of *gltA* determined via quantitative real-time PCR (qRT-PCR) after 3 or 6 h of growth. Data are the average ($n = 3$) fold changes relative to the wild type (wild type = 1) with standard errors of the mean. An asterisk denotes a significant difference (*t* test, $P < 0.05$). (C) Growth of wild-type (closed circle), *fakA* mutant (open circle), *codY* mutant (closed square), and *fakA codY* mutant (open square) strains. Data are the averages ($n = 3$) with standard deviations from representative experiments. An asterisk indicates significance ($P < 0.05$) between WT and *codY* mutant at hours 2, 3, 9, 10, and 12 only, while # identifies difference between the *fakA* and *fakA codY* mutants at all time points. (D) Transcript levels of *ilvD* determined via qRT-PCR at 3 or 6 h of growth. Data are the average ($n = 3$) fold changes relative to the wild type (wild type = 1) with standard errors of the mean. An asterisk denotes a significant difference (*t* test, $P < 0.05$).

This highlights the importance of the production of α-ketoglutarate via glutamate and amino acids that can be converted to glutamate as an important provider of carbon in complex media upon glucose consumption that is necessary for growth of both wild-type and the *fakA* mutant strains.

DISCUSSION

While FakA is involved in the utilization of exogenous fatty acids, we provide data that the function of FakA extends into maintaining metabolic homeostasis (Fig. 10). In the absence of FakA, we observed an altered acetate switch, redox state, and changes in key metabolites, as well as intracellular amino acid pools when grown in complex laboratory media, providing a snapshot of the metabolic state of the cell during growth. The apparent shift in global metabolism observed in the *fakA* mutant results in an increased NAD^+/NADH ratio inside the cell. We also provide evidence supporting the FakA-dependent activity of CcpA, as shown through the altered transcription of *gltA* observed in the *fakA* mutant. It should be noted that we have recently reported that FakA is an activator of the SaeRS two-component system (30), while another group demonstrated that CodY binds to the *sae* P1 promoter (39). Thus, it was reasonable to postulate that Sae would be important for the growth phenotype observed in the *fakA* mutant. However, in our previous study we did not note a growth difference between the *fakA* mutant and the *fakA sae* combination mutant. We reexamined this under the growth conditions here and again observed no contribution of *sae* to the enhanced growth of the *fakA* mutant (data not shown), demonstrating the ability of FakA to affect multiple cellular networks.

The details of glucose/acetate metabolism have been well described for *S. aureus*, with acetate reassimilated post-glucose consumption. Acetate is primarily generated by the Pta-AckA pathway, and acetate consumption is thought to be mediated by AscA,

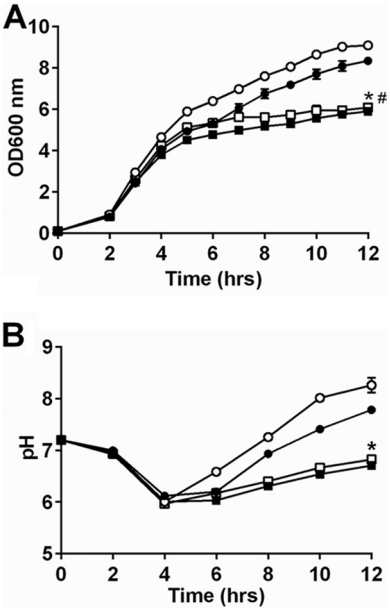

FIG 9 (A) Growth of wild-type (closed circle), *fakA* mutant (open circle), *gudB* mutant (closed square), and *fakA gudB* mutant (open square) strains. An asterisk denotes a significant difference ($P < 0.05$) for the wild type versus the *gudB* mutant at all points after 4 h, and # identifies difference for the *fakA* mutant versus the *fakA gudB* mutant for all time points after 2 h. (B) pH of culture media from panel A. Data are the averages ($n = 3$) with standard deviations from representative experiments. An asterisk denotes a significant difference (*t* test, $P < 0.05$) at all points for *gudB* mutants versus parent strains. All points have error bars, which may be smaller than symbols.

which converts acetate to acetyl-CoA. In support of this, both wild-type and the *fakA* mutant strains generated acetate until glucose exhaustion, at which point acetate was consumed, with the mutant depleting acetate at a higher rate (Fig. 1). Both strains depleted acetate by 12 h (Fig. 2C). As expected, we observed diminished levels of acetate in the *ackA* mutants, indicating that the Pta-AckA pathway is the predominate pathway for acetate production in both strains. Contrary to the model, we observed the depletion of approximately 75% of the acetate produced in the absence of *acsA* (Fig. S2). Similarly to the wild type versus the *fakA* mutant, the deletion of *fakA* in the *acsA* mutant led to increased acetate consumption. While these data do not directly measure acetate conversion to acetyl-CoA, removal of acetate from the media clearly requires enzymes besides AscA. Together, these data provide evidence for an enzyme capable of compensating for the lack of AcsA. The identity of this enzyme is unknown; however, there is a putative AMP-binding enzyme (SAUSA300_2542, EC 6.2.1.1) that may be redundant with that of *acsA*. In addition, there is evidence in *Escherichia coli* that AckA can work in reverse (24, 25, 40), but the kinetics are not favorable at the concentrations produced by *S. aureus*. Also, acetate levels did not decrease in the *ackA* mutant (Fig. 2C), suggesting that this is not the case. The identification of the enzyme(s) responsible for acetate consumption in *S. aureus* and determination of whether AckA can act to consume acetate await further investigation.

Acetate is often thought to be a primary source of carbon for *S. aureus* post-glucose depletion, yet even strains that do not completely use acetate grow well. Another abundant nutrient source in TSB is peptides and amino acids, some of which can be shuttled into the TCA cycle due to GudB; therefore, the result that mutation of *gudB* alters growth post-glucose consumption is not surprising. Halsey et al. (13) recently showed that in chemically defined media, amino acids that can be converted to glutamate are an important source of carbon (13). This seems to be the case in complex media, such as TSB, as well. Indeed, the *gudB* and *fakA gudB* mutants entered stationary phase once glucose was consumed, demonstrating the importance of amino acids for *S. aureus* growth post-glucose consumption. This result highlights the importance of

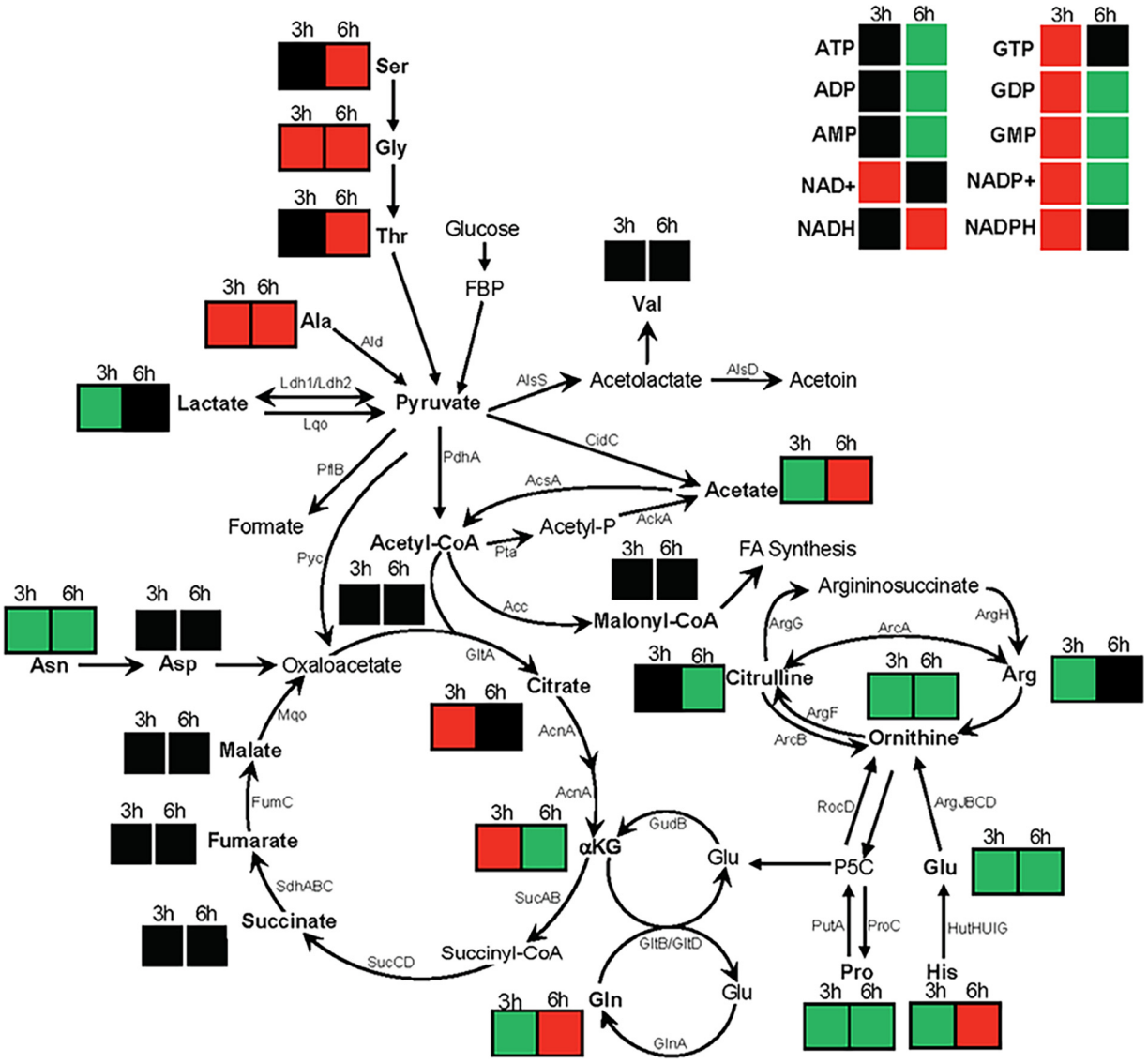

FIG 10 Relative change in intracellular concentrations of metabolites and their location in metabolism. Colors indicate either an increase (green box), decrease (red box), or no significant change (black box) at 3 or 6 h in the *fakA* mutant compared to in the wild type.

shuttling amino acids into the TCA cycle for growth of *S. aureus* despite an alternate energy source such as acetate. Furthermore, we hypothesize that the activity of glutamate dehydrogenase and the concomitant production of ammonia are necessary for the increased pH observed during the growth of wild-type and *fakA* strains.

We provide data suggesting a FakA-mediated effect on CcpA activity by using the expression of *gltA* (citrate synthase) as readout of CcpA activity. While *gltA* has been used as a marker for CcpA activity, the expression of this gene is dependent on more than just CcpA. Thus, one limitation for this experiment is that *fakA* alters *gltA* through other means. Furthermore, CcpA is activated by Hpr kinase, which is in turn activated by fructose-1,6-bisphosphate (FBP) (8). While we show that CcpA activity is affected by the lack of *fakA*, we did not measure levels of FBP in the *fakA* mutant. Thus, a change in steady-state FBP levels in *fakA* could be responsible for the altered CcpA activity suggested. Furthermore, Hpr is linked to the glucose phosphotransferase system (PTS), and changes in transport could affect Hpr, and subsequently CcpA, activity (8). More directed studies of the activity of CcpA in the context of FakA are needed to further characterize this relationship.

While regulation of *ilvD* is complex, it is used as an indicator mRNA for CodY activity. As expected, inactivation of *codY* increased transcription of *ilvD*, whereas no difference was observed in the *fakA* mutant alone. However, we observed decreased *ilvD* transcription in the *fakA codY* mutant compared to that in the *codY* mutant (Fig. 8D), indicating that in the absence of the repressor CodY, an additional activator is necessary for *ilvD* expression. Moreover, this proposed activator has reduced activity in the absence of FakA, and *ilvD* expression cannot be fully induced. The gene products *gcp* and *yeaZ* have been shown to repress *ilv-leu* transcription; however, the mechanism has not been identified (41, 42). Since these proteins repress *ilvD* expression, it is unlikely that they are the proteins by which FakA acts in the absence of CodY. It is possible that the decrease in *ilvD* expression in the *fakA codY* mutant compared to that in the *codY* mutant is not transcriptional and is the result of early transcription termination or mRNA stability. Recently, a report identified an attenuator peptide and termination loop structure, which is dependent on amino acid levels, in the 5′ untranslated region (UTR) of *ilvD* (39). The change in the concentration of amino acids could have effects on regulatory factors such as this attenuator peptide. However, the identification of the regulatory factor uncovered by our data remains to be elucidated.

Fatty acid biosynthesis begins with the conversion of acetyl-CoA to malonyl-CoA, which is then eventually converted to phospholipids for membrane incorporation (36). Due to its role in utilizing exogenous fatty acids, it was possible that fatty acid biosynthesis would be upregulated in the absence of *fakA*. We observed no difference in either intracellular malonyl-CoA levels or in the transcription of fatty acid biosynthesis genes, indicating that in complex media, the absence of *fakA* does not result in increased *de novo* fatty acid biosynthesis. This was not surprising, since it has been shown that exposure of *S. aureus* to a fatty acid-rich environment does not alter expression of the fatty acid biosynthesis pathway (43) and that exogenous fatty acids do not alter cellular malonyl-CoA levels (44). In support of this, our data demonstrate that the ability to use environmental fatty acids does not influence the endogenous synthesis pathway.

In this study, we have demonstrated a rewiring of *S. aureus* metabolism in response to the presence or absence of the fatty acid kinase. This alteration of metabolism involves changes in central metabolism, as well as pathways for amino acid utilization. Furthermore, these results, when combined with work previously done in our lab and by other groups, demonstrate an important link between fatty acid metabolism, central metabolism, and virulence factor regulation.

MATERIALS AND METHODS

Bacterial strains, plasmids, and growth conditions. The bacterial strains and plasmids used in this study are presented in Table 1. *Escherichia coli* strains were grown in lysogeny broth (LB) or on LB agar (15% [wt/vol]) supplemented with ampicillin (100 μg ml^{-1}) for antibiotic selection when necessary. *S. aureus* was grown in TSB supplemented with chloramphenicol (10 μg ml^{-1}) or erythromycin (5 μg ml^{-1}) when necessary. For analyzing bacterial growth, *S. aureus* overnight cultures were initially inoculated to an optical density at 600 nm of 0.1 in TSB without dextrose, which was supplemented with 14 mM glucose and filter sterilized. Unless otherwise stated, cultures were incubated at 37°C with shaking at 250 rpm in a flask-to-medium ratio of 10:1. Growth was measured using optical density at 600 nm readings or by assessing the number of CFU per milliliter on TSB with 15% (wt/vol) agar.

Measurement of glucose and acetate concentrations in the culture medium. Aliquots of bacterial cultures (1.0 ml) were pelleted at 21,130 $\times$ *g* for 5 min. Supernatants were decanted and stored at −20°C until analysis was performed. Acetate and glucose was quantified using kits purchased from R-Biopharm (Washington, MO) according to the manufacturer's protocol.

Measurement of urease activity. Urease activity was determined according to the method of Onal Okyay et al. (45), with minor adjustments. Briefly, overnight cultures were inoculated to an optical density at 600 nm of 0.5 in Stuart's broth (46). The suspensions were incubated at 37°C with shaking at 250 rpm for 24 h. Following incubation, the suspensions were centrifuged at 3,160 $\times$ *g* for 10 min and the supernatants were removed and scanned. Optical density scans ranging from 400 nm to 600 nm were performed at time of inoculation and after 3, 6, and 24 h of growth using a Spark 10M plate reader (Tecan Group Ltd., Mannedorf, Switzerland). Optical density values at a wavelength of 560 nm as a measure of urease activity were compared using a medium blank.

Production of *S. aureus* mutants. *S. aureus* transposon mutants are listed in Table 1 and were obtained from BEI Resources. Bacteriophage ϕ11 were propagated on mutants containing the desired transposon by combining 5 ml of TSB with 5 ml phage buffer (in 500 ml water, as follows: 6.47 g

TABLE 1 Strains, plasmids, and oligonucleotides

Strain, plasmid, or oligonucleotide	Relevant characteristic(s)[a]	Source or reference
Strains		
RN4220	Highly transformable *S. aureus*	52
AH1263	USA300 CA-MRSA strain LAC without LAC-p03	53
JLB2	AH1263 Δ*fakA*	27
JLB113	AH1263 *ccpA*::*tetL*	12
JLB114	AH1263 Δ*fakA ccpA*::*tetL*	This study
JLB127	AH1263 *ackA*::NΣ	This study
JLB128	AH1263 Δ*fakA ackA*::NΣ	This study
JLB132	AH1263 *ureB*::NΣ	This study
JLB133	AH1263 Δ*fakA ureB*::NΣ	This study
JLB158	AH1263 *gudB*::NΣ	This study
JLB159	AH1263 Δ*fakA gudB*::NΣ	This study
NE385	Source of *acsA*::NΣ	54
NE1397	Source of *alsS*::NΣ	54
NE1642	Source of *ureB*::NΣ	54
KB8007	JE2-Δ*ackA*::*ermB*; Em^r	33
JLB165	AH1263 *codY*::NΣ	This study
JLB166	AH1263 Δ*fakA codY*::NΣ	This study
NE1518	Source of *gudB*::NΣ	54
NE1555	Source of *codY*::NΣ	54
NE1670	Source of *ccpA*::NΣ	54
NE1923	Source of *ldh1*::NΣ	54
NE1816	Source of *ldh2*::NΣ	54
JLB115	AH1263 *saeR*::NΣ	30
JLB116	AH1263 Δ*fakA saeR*::NΣ	30
JLB115	AH1263 *acsA*::NΣ	This study
JLB116	AH1263 Δ*fakA acsA*::NΣ	This study
JLB188	AH1263 *ldh1*::NΣ	This study
JLB189	AH1263 Δ*fakA ldh1*::NΣ	This study
JLB196	AH1263 *ldh2*::NΣ	This study
JLB197	AH1263 Δ*fakA ldh2*::NΣ	This study
JLB135	AH1263 *alsS*::NΣ	This study
JLB136	AH1263 Δ*fakA alsS*::NΣ	This study
Plasmids		
pJB185	Promoterless codon-optimized *lacZ*, Amp/Cm^r	30
pJB165	*fakA* complement, Amp/Cm^r	27
pZD3	P_{ure}-*lacZ* reporter, Amp/Cm^r	This study
Oligonucleotides		
RT_ilvD_F	GGACCAGGTATGCCTGAAAT	This study
RT_ilvD_R	GGGGAAATATGACCAACTGC	This study
RT_gltA_F	TGGAAAAACGTATGGCAGAA	This study
RT_gltA_R	CCATCCTGCAGAACGACTTA	This study
RT-sigA-F	AACTGAATCCAAGTGATCTTAGTG	55
RT-sigA-R	TCATCACCTTGTTCAATACGTTTG	55
Purease-F2	aatgaattcGATGATGCTACCTACAATAGCCGCTA	This study
Purease-R2	ggacgtcgacCCAATTTCATATTAGATACAATTTACAAAATT	This study
CNK61	GATATGCCATTTCCAACTGTCG	This study
CNK63	GCTGCAAGTTGATCCATAGAGG	This study

[a]Antibiotic resistance abbreviations used: Amp/Cm^r, ampicillin and chloramphenicol resistant; Em^r, erythromycin resistant; *tetL*, tetracycline resistance gene. Oligonucleotide sequences are provided in the 5′-to-3′ orientation. Lowercase indicates nonhomologous sequences added for cloning purposes. CA-MRSA, community-associated methicillin-resistant *Staphylococcus aureus*.

glycerol-2-phosphate, disodium salt, 0.06 g $MgSO_4$, 2.4 g NaCl, and 0.5 g gelatin), 100 μl ϕ11 ($\sim 1 \times 10^{10}$ bacteriophage), and 100 μl of overnight donor strain, mixed by inversion, and incubated statically at room temperature overnight. The resulting ϕ11 bacteriophage was then filter sterilized using a 0.45-μm filter syringe and stored at 4°C until use. Transductions were performed as described previously (47). Genotypes were confirmed in transductants via PCR.

Analysis of β-galactosidase activity. To construct pZD3, primers Purease-F2 (aatgaattcGATGATGC TACCTACAATAGCCGCTA) and Purease-R2 (ggacgtcgacCCAATTTCATATTAGATACAATTTACAAAATT) were used to amplify the promoter region of *ureA* from the AH1263 chromosome. The resulting PCR fragment was digested with EcoRI and SalI and ligated into the same sites of pJB185 to produce pZD3. β-Galactosidase activity was determined as previously described (30). Briefly, 1 ml of bacterial culture was collected after 3 or 6 h of growth. Cells were pelleted, resuspended in 1.2 ml Z-buffer (60 mM Na_2HPO_4, 40 mM NaH_2PO_4, 10 mM KCl, 1 mM $MgSO_4$, and 3.4 ml β-mercaptoethanol) and lysed using a FastPrep-24

5G homogenizer (MP Biomedicals), according to the manufacturer's recommended settings for *S. aureus* cells. β-Galactosidase activity was determined by adding 140 μl of *ortho*-nitrophenyl-β-galactosidase (ONPG) (4 mg ml^{-1} [wt/vol]) to 700 μl of cell lysates and allowing reaction to turn slightly yellow at an absorbance at 420 nm of less than 1.0 at 37°C. The reaction was stopped with 200 μl of 1 M sodium bicarbonate, and then absorbance was measured at 420 nm. β-Galactosidase activity was determined based on protein concentration using a Bradford assay with Bio-Rad protein concentration reagent and reported as modified Miller units.

Reverse transcription-quantitative real-time PCR. RNA was extracted using an RNeasy minikit (Qiagen) after 3 and 6 h of growth in TSB plus 14 mM glucose. The isolated RNA was treated with a DNA-free kit (Ambion) to remove DNA contamination. RNA samples were quantified using a NanoDrop One instrument (Thermo Fisher Scientific). RNA was standardized to 500 ng and used for cDNA synthesis using a QuantiTect reverse transcription kit (Qiagen). cDNA was diluted 1:10 and used as the template DNA for quantitative PCR, using FastStart essential DNA Green master mix in a LightCycler 96 system (Roche). Data were calculated and analyzed according to Livak et al. (48). Data are the average from biological triplicates each run as technical duplicates. Primers CNK61 (GATATGCCATTTCCAACTGTCG) and CNK63 (GCTGCAAGTTGATCCATAGAGG) were used to amplify *fabH*, RT-*ilvD*-F (GGACCAGGTATGCCTGA AAT) and RT-*ilvD*-R (GGGGAAATATGACCAACTGC) were used to amplify *ilvD*, and RT-*gltA*-F (TGGAAAAA CGTATGGCAGAA) and RT-*gltA*-R (CCATCCTGCAGAACGACTTA) were used to amplify *gltA*. Data were standardized to *sigA* (*rpoD*) using primers RT-*sigA*-F (AACTGAATCCAAGTGATCTTAGTG) and RT-*sigA*-R (TCATCACCTTGTTCAATACGTTTG), as this has been shown to be a good calibrator previously (49, 50), and we typically observed less than one threshold cycle (C_T) difference between strains.

Cell collection and metabolite sample preparation for metabolite analysis. All glassware was triple washed with high-performance liquid chromatography (HPLC)-grade water, then three times with HPLC-grade acetone, and, finally, three times more with water. Overnight cultures of AH1263 and JLB2 were diluted to an optical density at 600 nm (OD_{600}) of 0.1 in TSB with 14 mM glucose at a 1:10 medium-to-flask ratio and incubated at 37°C with shaking at 250 rpm. Four biological replicates were examined. Samples were removed at 3 or 6 h postinoculation and centrifuged to pellet the cells. After centrifugation, supernatants were separated into 1-ml aliquots and frozen by submersion in liquid nitrogen. The cell pellets were washed in cold phosphate-buffered saline (PBS), aliquoted, and recentrifuged and had PBS removed, with immediate submersion in liquid nitrogen. All samples were stored at −80°C until analyzed. For cell pellets, an additional tube was used for cell quantification and protein content determination using a Bradford assay with Bio-Rad protein concentration reagent. Samples were processed using LC-MS/MS, as previously described (51). The adenylate energy charge was calculated as (ATP + 0.5ADP)/(AMP + ATP + ADP), as previously described (37). Data were analyzed using a paired Student *t* test, where $P < 0.05$ was considered statistically significant.

Statistical analyses. All statistical analyses were performed using Prism, version 6 (GraphPad). Statistical significance was determined using an unpaired *t* test with the Holm-Sidak method for multiple comparisons, where $P < 0.05$ was considered statistically significant unless otherwise stated. As stated above, mass spectrometry statistics were analyzed by the Southeast Center for Integrated Metabolomics (SECIM) Core using a *t* test in Microsoft Excel and revalidated using Prism.

SUPPLEMENTAL MATERIAL

Supplemental material for this article may be found at https://doi.org/10.1128/JB.00345-18.

SUPPLEMENT FILE 1, PDF file, 0.1 MB.

ACKNOWLEDGMENTS

We thank Paul Fey at the University of Nebraska Medical Center for providing strains and Kelly Rice at the University of Florida for thoughtful discussion. In addition, we are grateful for the work of Christopher Petucci, along with that of members of the Southeast Center for Integrated Metabolomics, for mass spectrometry analysis.

Research reported in this publication was supported by the National Institute of Allergy and Infectious Diseases under award number R01AI121073 (to J.L.B.).

REFERENCES

1. Lowy FD. 1998. *Staphylococcus aureus* infections. N Engl J Med 339:520–532. https://doi.org/10.1056/NEJM199808203390806.
2. Somerville GA. 2009. At the crossroads of bacterial metabolism and virulence factor synthesis in staphylocci. Microbiol Mol Biol Rev 73:233–248. https://doi.org/10.1128/MMBR.00005-09.
3. Richardson AR, Somerville GA, Sonenshein AL. 2015. Regulating the intersection of metabolism and pathogenesis in Gram-positive bacteria. Microbiol Spectr 3. https://doi.org/10.1128/microbiolspec.MBP-0004-2014.
4. Pohl K, Francois P, Stenz L, Schlink F, Geiger T, Herbert S, Goerke C, Schrenzel J, Wolz C. 2009. CodY in *Staphylococcus aureus*: a regulatory link between metabolism and virulence gene expression. J Bacteriol 191:2953–2963. https://doi.org/10.1128/JB.01492-08.
5. Görke B, Stulke J. 2008. Carbon catabolite repression in bacteria: many ways to make the most out of nutrients. Nat Rev Microbiol 6:613–624. https://doi.org/10.1038/nrmicro1932.
6. Sonenshein AL. 2007. Control of key metabolic intersections in *Bacillus subtilis*. Nat Rev Microbiol 5:917–927. https://doi.org/10.1038/nrmicro1772.
7. Deutscher J, Kuster E, Bergstedt U, Charrier V, Hillen W. 1995. Protein kinase-dependent HPr/CcpA interaction links glycolytic activity to car-

bon catabolite repression in gram-positive bacteria. Mol Microbiol 15:1049–1053. https://doi.org/10.1111/j.1365-2958.1995.tb02280.x.
8. Deutscher J, Herro R, Bourand A, Mijakovic I, Poncet S. 2005. P-Ser-HPr—a link between carbon metabolism and the virulence of some pathogenic bacteria. Biochim Biophys Acta 1754:118–125. https://doi.org/10.1016/j.bbapap.2005.07.029.
9. Sadykov MR, Hartmann T, Mattes TA, Hiatt M, Jann NJ, Zhu Y, Ledala N, Landmann R, Herrmann M, Rohde H, Bischoff M, Somerville GA. 2011. CcpA coordinates central metabolism and biofilm formation in *Staphylococcus epidermidis*. Microbiology 157:3458–3468. https://doi.org/10.1099/mic.0.051243-0.
10. Lopez JM, Thoms B. 1977. Role of sugar uptake and metabolic intermediates on catabolite repression in *Bacillus subtilis*. J Bacteriol 129:217–224.
11. Seidl K, Muller S, Francois P, Kriebitzsch C, Schrenzel J, Engelmann S, Bischoff M, Berger-Bachi B. 2009. Effect of a glucose impulse on the CcpA regulon in *Staphylococcus aureus*. BMC Microbiol 9:95. https://doi.org/10.1186/1471-2180-9-95.
12. Nuxoll AS, Halouska SM, Sadykov MR, Hanke ML, Bayles KW, Kielian T, Powers R, Fey PD. 2012. CcpA regulates arginine biosynthesis in *Staphylococcus aureus* through repression of proline catabolism. PLoS Pathog 8:e1003033. https://doi.org/10.1371/journal.ppat.1003033.
13. Halsey CR, Lei S, Wax JK, Lehman MK, Nuxoll AS, Steinke L, Sadykov M, Powers R, Fey PD. 2017. Amino acid catabolism in *Staphylococcus aureus* and the function of carbon catabolite repression. mBio 8:e01434-16. https://doi.org/10.1128/mBio.01434-16.
14. Ratnayake-Lecamwasam M, Serror P, Wong KW, Sonenshein AL. 2001. *Bacillus subtilis* CodY represses early-stationary-phase genes by sensing GTP levels. Genes Dev 15:1093–1103. https://doi.org/10.1101/gad.874201.
15. Brinsmade SR, Kleijn RJ, Sauer U, Sonenshein AL. 2010. Regulation of CodY activity through modulation of intracellular branched-chain amino acid pools. J Bacteriol 192:6357–6368. https://doi.org/10.1128/JB.00937-10.
16. Brinsmade SR. 2017. CodY, a master integrator of metabolism and virulence in Gram-positive bacteria. Curr Genet 63:417–425. https://doi.org/10.1007/s00294-016-0656-5.
17. Roux A, Todd DA, Velazquez JV, Cech NB, Sonenshein AL. 2014. CodY-mediated regulation of the *Staphylococcus aureus* Agr system integrates nutritional and population density signals. J Bacteriol 196:1184–1196. https://doi.org/10.1128/JB.00128-13.
18. Montgomery CP, Boyle-Vavra S, Roux A, Ebine K, Sonenshein AL, Daum RS. 2012. CodY deletion enhances in vivo virulence of community-associated methicillin-resistant *Staphylococcus aureus* clone USA300. Infect Immun 80:2382–2389. https://doi.org/10.1128/IAI.06172-11.
19. Seidl K, Stucki M, Ruegg M, Goerke C, Wolz C, Harris L, Berger-Bachi B, Bischoff M. 2006. *Staphylococcus aureus* CcpA affects virulence determinant production and antibiotic resistance. Antimicrob Agents Chemother 50:1183–1194. https://doi.org/10.1128/AAC.50.4.1183-1194.2006.
20. Majerczyk CD, Sadykov MR, Luong TT, Lee C, Somerville GA, Sonenshein AL. 2008. *Staphylococcus aureus* CodY negatively regulates virulence gene expression. J Bacteriol 190:2257–2265. https://doi.org/10.1128/JB.01545-07.
21. Majerczyk CD, Dunman PM, Luong TT, Lee CY, Sadykov MR, Somerville GA, Bodi K, Sonenshein AL. 2010. Direct targets of CodY in *Staphylococcus aureus*. J Bacteriol 192:2861–2877. https://doi.org/10.1128/JB.00220-10.
22. Mlynek KD, Sause WE, Moormeier DE, Sadykov MR, Hill KR, Torres VJ, Bayles KW, Brinsmade SR. 2018. Nutritional regulation of the Sae two-component system by CodY in *Staphylococcus aureus*. J Bacteriol 200:e00012-18. https://doi.org/10.1128/JB.00012-18.
23. Rose IA, Grunberg-Manago M, Korey SR, Ochoa S. 1954. Enzymatic phosphorylation of acetate. J Biol Chem 211:737–756.
24. Brown TD, Jones-Mortimer MC, Kornberg HL. 1977. The enzymic interconversion of acetate and acetyl-coenzyme A in *Escherichia coli*. J Gen Microbiol 102:327–336. https://doi.org/10.1099/00221287-102-2-327.
25. Starai VJ, Escalante-Semerena JC. 2004. Acetyl-coenzyme A synthetase (AMP forming). Cell Mol Life Sci 61:2020–2030. https://doi.org/10.1007/s00018-004-3448-x.
26. Wolfe AJ. 2005. The acetate switch. Microbiol Mol Biol Rev 69:12–50. https://doi.org/10.1128/MMBR.69.1.12-50.2005.
27. Bose JL, Daly SM, Hall PR, Bayles KW. 2014. Identification of the *Staphylococcus aureus vfrAB* operon, a novel virulence factor regulatory locus. Infect Immun 82:1813–1822. https://doi.org/10.1128/IAI.01655-13.
28. Parsons JB, Broussard TC, Bose JL, Rosch JW, Jackson P, Subramanian C, Rock CO. 2014. Identification of a two-component fatty acid kinase responsible for host fatty acid incorporation by *Staphylococcus aureus*. Proc Natl Acad Sci U S A 111:10532–10537. https://doi.org/10.1073/pnas.1408797111.
29. Lopez MS, Tan IS, Yan D, Kang J, McCreary M, Modrusan Z, Austin CD, Xu M, Brown EJ. 2017. Host-derived fatty acids activate type VII secretion in *Staphylococcus aureus*. Proc Natl Acad Sci U S A 114:11223–11228. https://doi.org/10.1073/pnas.1700627114.
30. Krute CN, Rice KC, Bose JL. 2017. VfrB is a key activator of the *Staphylococcus aureus* SaeRS two-component system. J Bacteriol 199:e00828-16.
31. Sabirova JS, Hernalsteens JP, De Backer S, Xavier BB, Moons P, Turlej-Rogacka A, De Greve H, Goossens H, Malhotra-Kumar S. 2015. Fatty acid kinase A is an important determinant of biofilm formation in *Staphylococcus aureus* USA300. BMC Genomics 16:861. https://doi.org/10.1186/s12864-015-1956-8.
32. Thomas VC, Sadykov MR, Chaudhari SS, Jones J, Endres JL, Widhelm TJ, Ahn JS, Jawa RS, Zimmerman MC, Bayles KW. 2014. A central role for carbon-overflow pathways in the modulation of bacterial cell death. PLoS Pathog 10:e1004205. https://doi.org/10.1371/journal.ppat.1004205.
33. Sadykov MR, Thomas VC, Marshall DD, Wenstrom CJ, Moormeier DE, Widhelm TJ, Nuxoll AS, Powers R, Bayles KW. 2013. Inactivation of the Pta-AckA pathway causes cell death in *Staphylococcus aureus*. J Bacteriol 195:3035–3044. https://doi.org/10.1128/JB.00042-13.
34. Somerville GA, Said-Salim B, Wickman JM, Raffel SJ, Kreiswirth BN, Musser JM. 2003. Correlation of acetate catabolism and growth yield in Staphylococcus aureus: implications for host-pathogen interactions. Infect Immun 71:4724–4732. https://doi.org/10.1128/IAI.71.8.4724-4732.2003.
35. Heath RJ, White SW, Rock CO. 2001. Lipid biosynthesis as a target for antibacterial agents. Prog Lipid Res 40:467–497. https://doi.org/10.1016/S0163-7827(01)00012-1.
36. Parsons JB, Rock CO. 2013. Bacterial lipids: metabolism and membrane homeostasis. Prog Lipid Res 52:249–276. https://doi.org/10.1016/j.plipres.2013.02.002.
37. Atkinson DE, Walton GM. 1967. Adenosine triphosphate conservation in metabolic regulation. Rat liver citrate cleavage enzyme. J Biol Chem 242:3239–3241.
38. Sonenshein AL. 2005. CodY, a global regulator of stationary phase and virulence in Gram-positive bacteria. Curr Opin Microbiol 8:203–207. https://doi.org/10.1016/j.mib.2005.01.001.
39. Kaiser JC, King AN, Grigg JC, Sheldon JR, Edgell DR, Murphy MEP, Brinsmade SR, Heinrichs DE. 2018. Repression of branched-chain amino acid synthesis in *Staphylococcus aureus* is mediated by isoleucine via CodY, and by a leucine-rich attenuator peptide. PLoS Genet 14:e1007159. https://doi.org/10.1371/journal.pgen.1007159.
40. Enjalbert B, Millard P, Dinclaux M, Portais JC, Letisse F. 2017. Acetate fluxes in Escherichia coli are determined by the thermodynamic control of the Pta-AckA pathway. Sci Rep 7:42135. https://doi.org/10.1038/srep42135.
41. Lei T, Yang J, Ji Y. 2015. Determination of essentiality and regulatory function of staphylococcal YeaZ in branched-chain amino acid biosynthesis. Virulence 6:75–84. https://doi.org/10.4161/21505594.2014.986415.
42. Lei T, Yang J, Zheng L, Markowski T, Witthuhn BA, Ji Y. 2012. The essentiality of staphylococcal Gcp is independent of its repression of branched-chain amino acids biosynthesis. PLoS One 7:e46836. https://doi.org/10.1371/journal.pone.0046836.
43. Balemans W, Lounis N, Gilissen R, Guillemont J, Simmen K, Andries K, Koul A. 2010. Essentiality of FASII pathway for *Staphylococcus aureus*. Nature 463:E3; discussion E4. https://doi.org/10.1038/nature08667.
44. Parsons JB, Frank MW, Subramanian C, Saenkham P, Rock CO. 2011. Metabolic basis for the differential susceptibility of Gram-positive pathogens to fatty acid synthesis inhibitors. Proc Natl Acad Sci U S A 108:15378–15383. https://doi.org/10.1073/pnas.1109208108.
45. Onal Okyay T, Frigi Rodrigues D. 2013. High throughput colorimetric assay for rapid urease activity quantification. J Microbiol Methods 95:324–326. https://doi.org/10.1016/j.mimet.2013.09.018.
46. Stuart CA, Vanstratum E, Rustigian R. 1945. Further studies on urease production by *Proteus* and related organisms. J Bacteriol 49:437–444.
47. Krausz KL, Bose JL. 2016. Bacteriophage transduction in *Staphylococcus aureus*: broth-based method. Methods Mol Biol 1373:63–68. https://doi.org/10.1007/7651_2014_185.
48. Livak KJ, Schmittgen TD. 2001. Analysis of relative gene expression data using real-time quantitative PCR and the 2(−delta delta C(T)) method. Methods 25:402–408. https://doi.org/10.1006/meth.2001.1262.
49. Lewis AM, Rice KC. 2016. Quantitative real-time PCR (qPCR) workflow for analyzing *Staphylococcus aureus* gene expression. Methods Mol Biol 1373:143–154. https://doi.org/10.1007/7651_2014_193.
50. Moormeier DE, Endres JL, Mann EE, Sadykov MR, Horswill AR, Rice KC, Fey PD, Bayles KW. 2013. Use of microfluidic technology to analyze gene expr. during *Staphylococcus aureus* biofilm formation reveals distinct

physiological niches. Appl Environ Microbiol 79:3413–3424. https://doi.org/10.1128/AEM.00395-13.
51. Mogen AB, Carroll RK, James KL, Lima G, Silva D, Culver JA, Petucci C, Shaw LN, Rice KC. 2017. *Staphylococcus aureus* nitric oxide synthase (saNOS) modulates aerobic respiratory metabolism and cell physiology. Mol Microbiol 105:139–157. https://doi.org/10.1111/mmi.13693.
52. Kreiswirth BN, Löfdahl S, Betley MJ, O'Reilly M, Schlievert PM, Bergdoll MS, Novick RP. 1983. The toxic shock syndrome exotoxin structural gene is not detectably transmitted by a prophage. Nature 305:709–712. https://doi.org/10.1038/305709a0.
53. Boles BR, Thoendel M, Roth AJ, Horswill AR. 2010. Identification of genes involved in polysaccharide-independent *Staphylococcus aureus* biofilm formation. PLoS One 5:e10146. https://doi.org/10.1371/journal.pone.0010146.
54. Fey PD, Endres JL, Yajjala VK, Widhelm TJ, Boissy RJ, Bose JL, Bayles KW. 2013. A genetic resource for rapid and comprehensive phenotype screening of nonessential *Staphylococcus aureus* genes. mBio 4:e00537-12. https://doi.org/10.1128/mBio.00537-12.
55. Lehman MK, Bose JL, Sharma-Kuinkel BK, Moormeier DE, Endres JL, Sadykov MR, Biswas I, Bayles KW. 2015. Identification of the amino acids essential for LytSR-mediated signal transduction in *Staphylococcus aureus* and their roles in biofilm-specific gene expression. Mol Microbiol 95:723–737. https://doi.org/10.1111/mmi.12902.